Pergamon

Tetrahedron: Asymmetry, Vol. 7, No. 4, pp. 1123-1136, 1996

0957-4166/96 $15.00 + 0.00

S0957-4166(96)00118-8

A Predictive Active Site Model for Cyclohexanone Monooxygenase Catalyzed Baeyer-Villiger Oxidations

Gianluca OTTOLINA,[1*] Giacomo CARREA,[1] Stefano COLONNA[2] and Andreas RÜCKEMANN[2]

[1]Istituto di Chimica degli Ormoni, C.N.R., Via Mario Bianco 9, 20131 Milano

[2]Istituto di Chimica Organica, Facoltà di Farmacia, Via Venezian 21, Milano, Italy,

Abstract. An extension to Baeyer-Villiger oxidations of the active site model previously developed (*Tetrahedron: Asymmetry*, **1995**, *6*, 1375) for the enantioselective sulfoxidation of organic sulfides catalyzed by cyclohexanone monooxygenase from *Acinetobacter* NCIMB 9871 is proposed. The model is based on cubic-space descriptors and can explain the stereoselectivity of the enzyme for about 40 different substrates.

Introduction.

Since its discovery in 1899, the Baeyer-Villiger reaction[1] has been used extensively in organic synthesis to convert ketones into esters or lactones. The enzyme catalyzed reaction has been introduced for synthesis more recently, and one of the most important enzymes used for this is cyclohexanone monooxygenase (CYMO) from *Acinetobacter* NCIMB 9871 (EC 1.14.13.22)[2] (**Scheme**). This enzyme has also been used for the asymmetric sulfoxidation of sulfides.[3]

Despite efforts made to determine the protein structure, there are still no tridimentional data for CYMO and this, of course, hampers use of this enzyme in synthesis. The stereochemical behavior of CYMO is substrate sensitive, and sometimes the results appear quite bizarre in comparison with the correspondent abiotic reaction. This emphasizes the need for an active site model able to explain and justify the data reported in the literature. Three models have been proposed so far[4-6], but none of them has been extensively checked.

During the course of our studies of enzymatic sulfoxidations, we proposed an active site model for CYMO which was tentatively applied also to a few Baeyer-Villiger reactions.[7] In the present study we also found that after some minor refinements, the active site model is valid and predictive for the stereochemical outcome of Baeyer-Villiger oxidation in general.

Approach, description and rules for application.

Tables I and **II** show the data collected from the literature about Baeyer-Villiger oxidations catalyzed by *Acinetobacter* NCIMB 9871. We did not include data from studies in which the enantiomeric purity of the products was low (ee ≤50%) or the attribution of the absolute configuration uncertain.

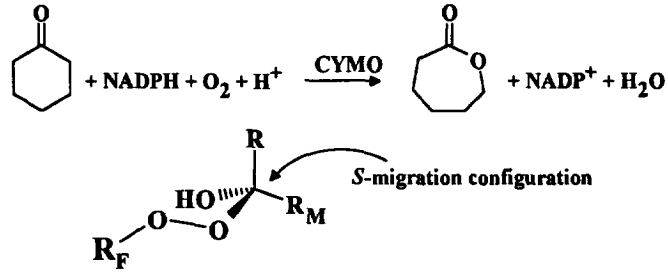

Scheme. Enzymatic Baeyer-Villiger intermediate (Criegee intermediate) for a generic substrate. R_M and R_F are representing respectively the migrating fragment and the flavin moiety.

Table I. CYMO-catalyzed Baeyer-Villiger oxidations.

Entry	Substrate	Product "Normal BV"	ee (%)	Yield (%)	Product "Reverse BV"	ee (%)	Yield (%)	Ref.
1	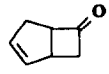	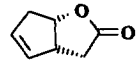	98	40	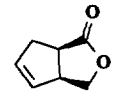	94	37	4, 16-18
2	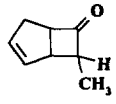	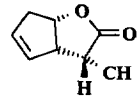	96	25	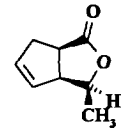	96	25	19-20
3	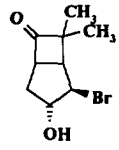	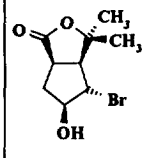	98	30				16, 19-20
4	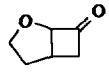	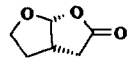	90	35	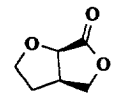	98	32	21
5	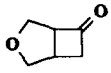	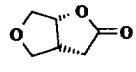	97	35	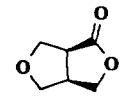	98	35	21
6	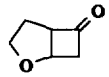	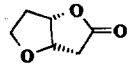	98	33	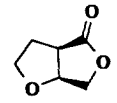	98	41	21
7	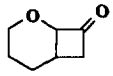	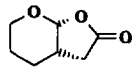	70	33	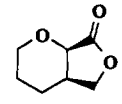	98	33	21
8	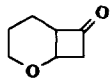	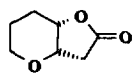	33	60	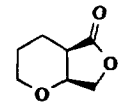	98	18	21

Table II. CYMO-catalyzed Baeyer-Villiger oxidations

Entry	Substrate	Product	e.e. (%)	Yield (%)	Ref.
9			80	62	5, 22
10			98	70	5, 22
11		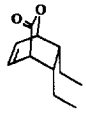	93	83	5, 22
12	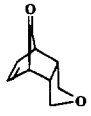	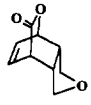	98	74	5, 22
13		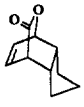	97	80	5, 22
14	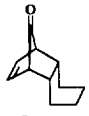	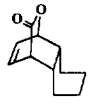	98	78	5, 22
15		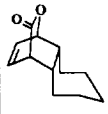	98	57	5, 22
16	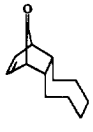	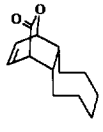	87	55	5, 22
17	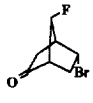	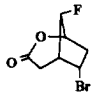	95		23
18	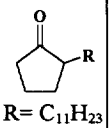 R= $C_{11}H_{23}$	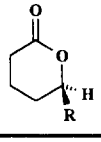	75	24	5, 8

Entry	Substrate	Product	e.e. (%)	Yield (%)	Ref.
19	R= C_9H_{19}	similar	80	20	5, 24
20	R= C_7H_{15}	similar	90	35	5, 24
21	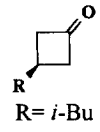 R= *i*-Bu	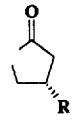	84	56	25
22	R= Bz	similar	82	57	25
23	R= 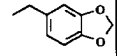	similar	95	83	25
24	R= CH_2OBz	similar	55	89	25
25	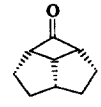	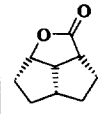	98	100	6
26	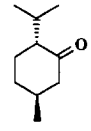	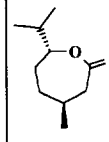		90	26
27	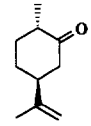	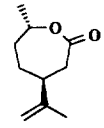		80	26
28	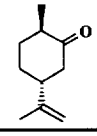	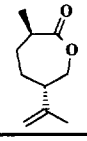		73	26

Table II. continued

Entry	Substrate	Product	ee (%)	Yield (%)	Ref.
29	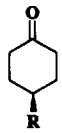 R= Me	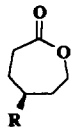	98	80	5, 27
30	R= Et	similar	98	84	5, 28
31	R= *n*-Pr	similar	98	80	5, 28
32	R= *t*-Bu	similar	98	17	5, 28
33	R= OMe	similar	75	76	5, 27
34	R= *i*-Pr	similar	98	60	5, 28
35	R= *n*-Bu	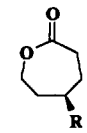	55	70	5
36	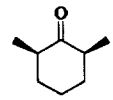	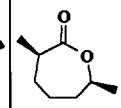	98	27	5, 27
37	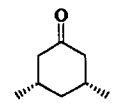	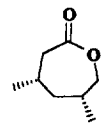	98	73	5, 27, 29
38	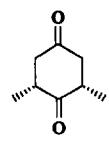	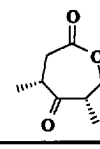	98	25	5, 27

Even though the majority of the oxidations were conducted with whole cells, in a few cases partially purified CYMO was also used. No substantial differences were observed in the enantiomeric excess and absolute configuration of the products for the two enzymatic preparations. In all cases, there was an hydrolytic enzyme (lactonase) and then, to prevent the hydrolysis of the products, different inhibitors were employed.[8,9]

The use of the "cubic space" approach,[10] based on enzyme substrate specificity, is perhaps the best way to describe the active site in the absence of any structural information about the enzyme. **Figure 1** displays the top, front and side views of the active site model, which basically resembles that proposed for sulfide enantioselective sulfoxidations.[7] The dimensions of the "sulfide" model, which was also able to predict the stereoselectivity of a few Baeyer-Villiger oxidations, delineated the minimum pocket volumes, and, to explain all the data in the literature concerning Baeyer-Villiger oxidations, an extension beneath the main pocket (M) was needed. Since the present model simply represents an enlargement of the earlier specifications, all previous interpretations of enzyme enantioselectivity with sulfides remain valid.

The strategy used for the determination of this enlargement traced that used for sulfides. For Baeyer-Villiger reactions, the energy of the intermediate substrate complex (Criegee intermediate or analogous structures) was minimized, using hydrogen as substituent (R_F) (see **Scheme**). The generally accepted rules for

Baeyer-Villiger oxidations affirm that the stereoelectronic requirements for the migration step are such that the bond of the migrating group (R_M) is antiperiplanar to both a nonbonding electron pair on oxygen[11] (the hydroxyl group in our case) and the O–O bond.[12] These requirements are used as a restraint in energy minimization.[13] The prochiral carbonyl group has two stereogenic faces suitable for attack by the 4a-hydroperoxide flavin, and this doubles the number of intermediates. In the chemical Baeyer-Villiger oxidation, the priority rules for the migrating group are strictly respected, but when the reaction is CYMO-catalyzed, in addition to the "normal" product one can in some cases obtain the "reverse" product. The priorities for the migrating group are not respected and this, again, doubles the number of intermediates.

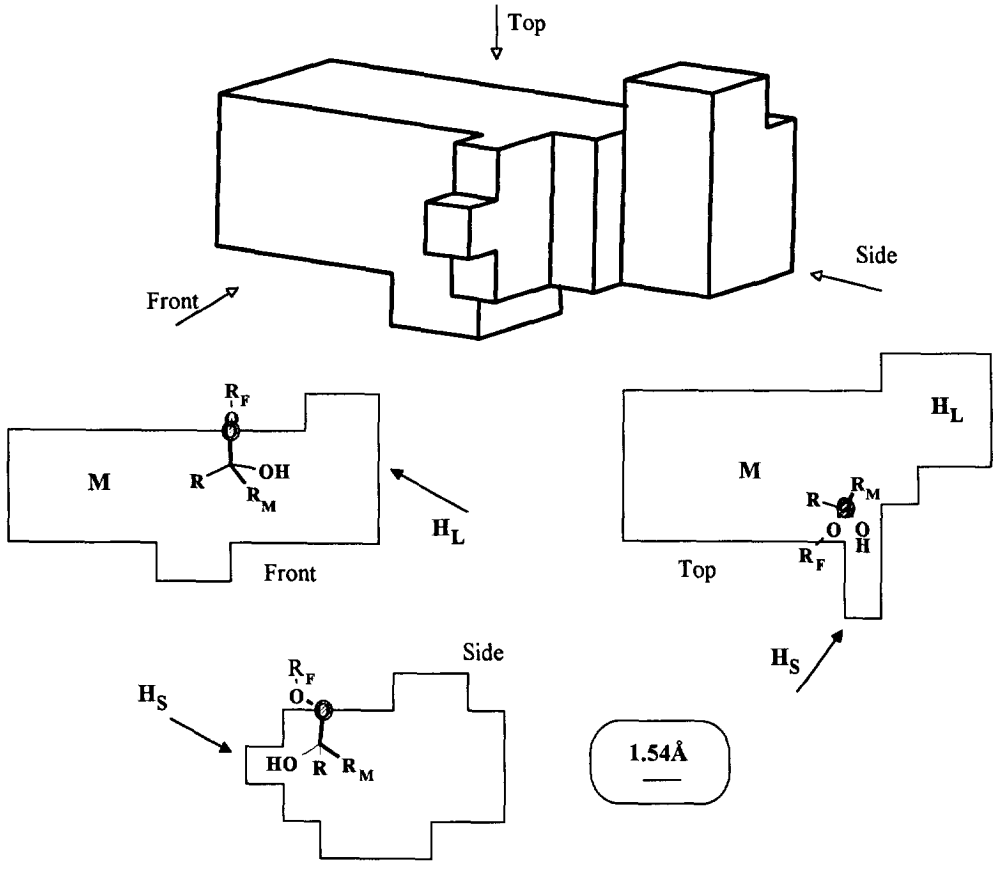

Figure 1. Active site model of CYMO. The catalytic region (oxygen) is encircled. The front, side and top views are also shown, together with the scale. The main (M), hydrophobic large (H_L) and hydrophobic small (H_S) pockets are depicted. It is also shown the correct arrangements of the Criegee intermediate inside the active site model

All the structures obtained were placed inside the "cage" representing the active site model. The positioning axis is the same used for sulfoxidation but, the S=O bond is replaced by the C–$O_{Peroxide}$ bond. In the

application of this model, a few guidelines must be respected in order to make predictions of the absolute configuration of the products:

Rule 1. The oxidized carbon atom must be placed in the catalytic site aligned along the C–$O_{Peroxide}$ axis, as if the reaction were taking place, and with the oxygen occupying the encircled region.

Rule 2. The migrating group (R_M) must be placed antiperiplanar to the O–O bond.

Rule 3. The hydroxyl group (C–OH) must be pointed toward the H_S pocket. If this is not possible, the reaction will not take place.

Rule 4. For a cyclic substrate the peroxide group will preferably be exo or equatorial.

It is worth keep in mind that this type of model cannot be used to predict the kinetic and quantitative features of the reactions such as V_{max}, K_m or yield, and also that the binding pockets must be viewed as real physical constraints that cannot be penetrated by the substrate.

Specific examples.

In this section the applications of the model to compounds **1-38** are shown. The compounds were divided into several groups for the sake of clarity and the full discussion is limited to one significant compound for each group, with only some considerations reported for the others.

7-Endo-methyl-bicyclo [3.2.0] hept-2-en-6-one **2** *and related compounds*

The title compound is part of a series of bicyclic ketones (**1-8; Table I**), which are quite interesting in the framework of enzymatic Baeyer-Villiger oxidations because, in addition to the normal migration (normal BV), there is an unusual migration (reverse BV), which is regio-inverted in respect to the abiotic reaction. Each enantiomer could theoretically be subjected to two different attacks (exo or endo) and two possible migrations (migration of the carbon C-5, "normal" or C-7, "reverse") and, thus, eight different intermediates can be hypothesized for this racemic compound. **Figure 2** depicts the four potential intermediates for the *S,S* enantiomer. Part *a* shows the top view of the exo-normal intermediate in the active site, with the C–$O_{Peroxide}$ bond beneath the oxygen (encircled) and with the hydroxyl group correctly pointing towards the H_S pocket. Part *b* shows the top view of the endo-normal intermediate in the active site with the hydroxyl group pointing towards the inside of the M pocket (see rule 3) and with the methyl group lying outside the active site, which indicates that this intermediate has to be rejected. Part *c* shows the top view of the exo-reverse intermediate. Again, the hydroxyl group is pointing towards the inside of the M pocket and the cyclopentene ring lies outside the active site and, thus, this structure too must be discarded. Finally part *d* shows the side view for the endo-reverse intermediate. Here, the entire intermediate is inside the active site, the hydroxyl group is pointing towards the H_S pocket and the peroxide fragment is endo. Since the exo intermediate is also possible (see part *a*), according to rule 4 this last structure has to be dropped.

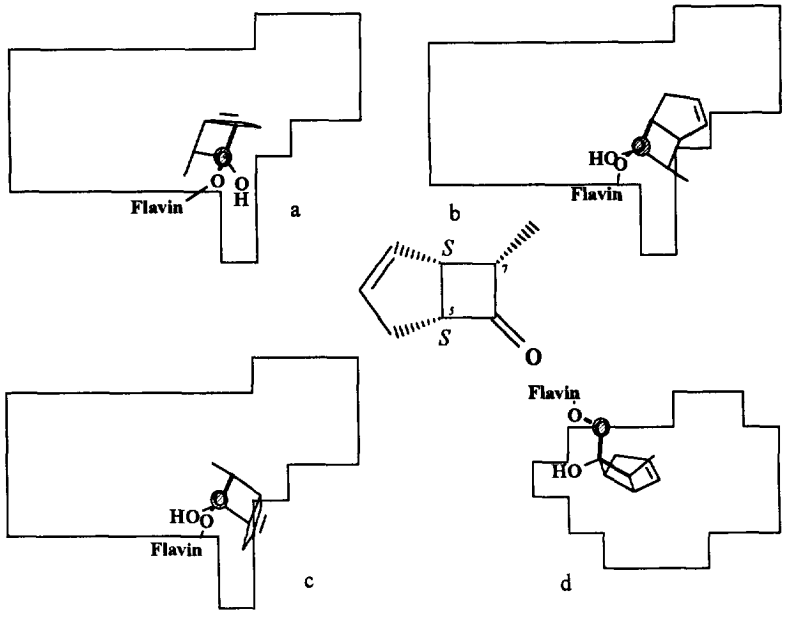

Figure 2. Sketches of the four possible intermediates of *S,S*-**2**.

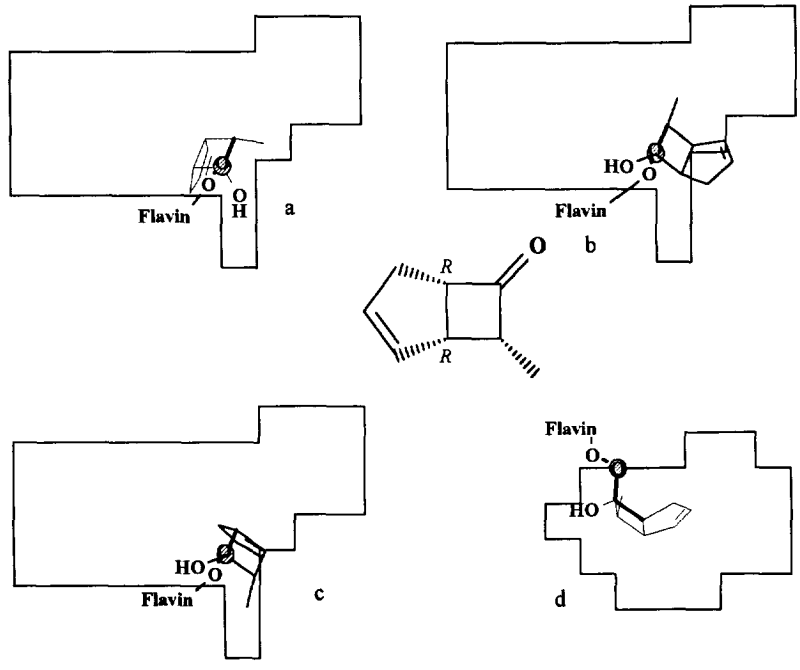

Figure 3. Sketches of the four possible intermediates of *R,R*-**2**.

An analogous discussion can be made for the *R,R* enantiomer, and **Figure 3** displays the four potential intermediates. Part *a* indicates the top view of the exo-reverse intermediate. The entire substrate is contained

within the active site, with the hydroxyl group in the right position. In part *b* (endo-reverse) and part *c* (exo-normal) the cyclopentene ring clearly lies outside the active site. Part *d* shows the side view of the endo-normal intermediate, which resides entirely inside the active site with the hydroxyl group directed towards the H_S pocket. As for the other enantiomer, the exo attachment is preferred to the endo and then the endo structure has to be discarded. Therefore, for this racemic compound, only two of eight possible intermediates can be accepted by the active site model and they are the ones that also give the products with the observed chirality. The "cubic space" model also sheds light on reverse Baeyer-Villiger oxidations. These reactions occur only when the normal migration is interdicted by steric factors whereas the other arrangements can fit inside the active site.

The results obtained with compounds **1** and **3-8** can be rationalized by a similar approach. Compound **3** is quite interesting because gives only one product with high ee. The addition of a methyl group at C-7 inverts the migratory priority and then the normal Baeyer-Villiger oxidation takes place, with the migration of C-7. Contrary to what is seen with compound **2**, the exo-reverse *S,S*-**3** intermediate does not fit the model because of the bulkiness of the substituents. The front view of the intermediate clearly shows that the hydroxyl group lies outside the active site (**Figure 4**, part *a*). For the reasons already discussed above for *S,S*-**2**, the endo-reverse and exo-normal intermediates must be discarded. For the *R,R* enantiomer, the exo-normal intermediate (exo-reverse for *R,R*-**2**) is the only feasible form to react (**Figure 4**, part *b*). With furan and pyran derivatives (entries **4-8**), the presence of an oxygen in the ring does not modify the behavior of the active site model, even though hydrogen bonding is possible in these cases. The low ee obtained with pyran derivatives can not be explained with the present model probably because it does not take into account polar effects and hydrogen bonding.

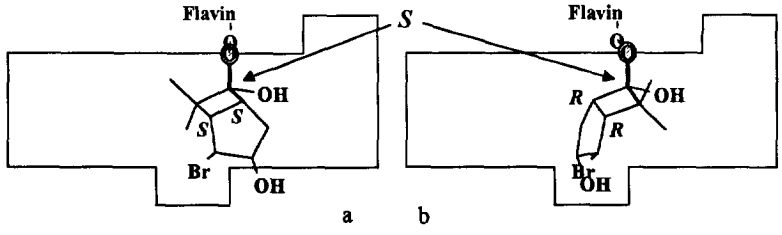

Figure 4. Front views of two possible intermediate of **3**.

Bicyclo [2.2.1] hept-2-en-7-one **9** *and related compounds*

Meso compounds **9-16** (**Table II**) are asymmetrized by cyclohexanone monooxygenase to give products with fairly high enantiomeric excess. Things here are simpler than those we have examined so far because there are only four possible intermediates for each compound. **Figure 5** illustrates the situation for compound **15**. The top view of the endo attack is shown in part *a*. In this case the hydroxyl group points towards the inside of the M pocket, and a ring moiety is outside the active site, which excludes this intermediate. Also the one

displayed in part *b* must be rejected, even if the hydroxyl group does point towards H_S, because there is an endo attack that is less favored than an exo attack (see rules), which would drive to the product with the wrong chirality. Part *c* shows the front view for the exo attachment intermediate. The structure lies partially outside

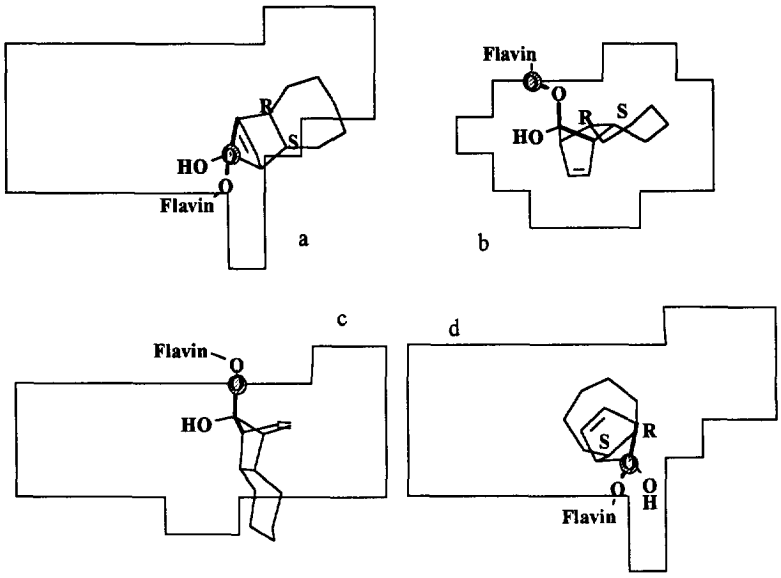

Figure 5. Sketches of the four possible intermediates of **15**.

the active site, with the hydroxyl group pointing towards the M pocket. Finally, in part *d*, the attack to the ketone gives a correctly positioned intermediate which yields the right enantiomer. Similar explanations hold for entries **9-14** and **16.**

3-Substituted cyclobutanones

Another interesting series of meso compounds is the cyclobutanones (**21-24**; **Table II**). As for the previously examined meso series, only four intermediates are possible. **Figure 6** depicts the intermediates for compound **22** and part *d* shows the intermediate which, according to our rules, explains the enzyme preference. In this case also it is important to stress that it is the exo/endo preference that dictates the right intermediate and, therefore, chirality of the product.

4-Substituted cyclohexanones

Great attention has been paid to this class of compounds (**29-35**; **Table II**), because we had to modify our previously developed active site model[7] to explain the behavior of compound **32**. The four possible intermediates of 4-*t*Bu cyclohexanone are shown in **Figure 7**. In parts *a* and *b*, the top views clearly show that

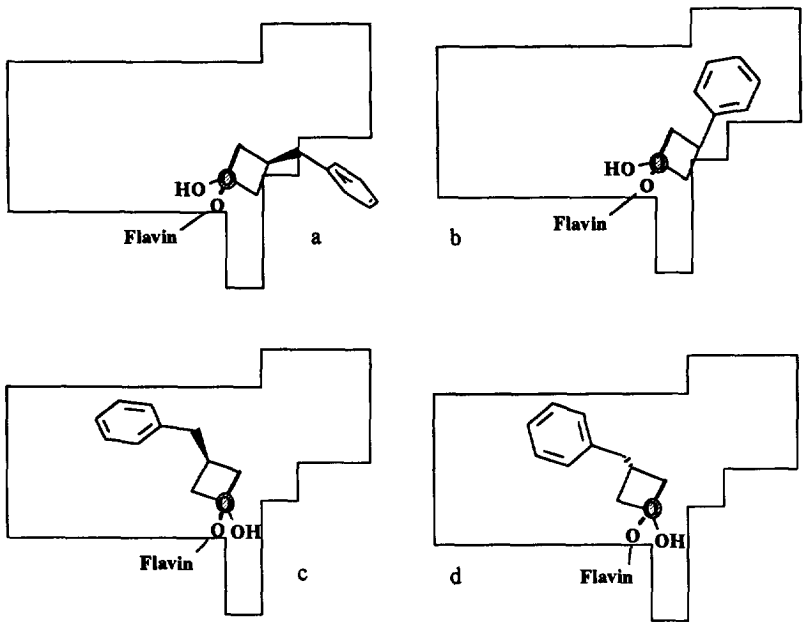

Figure 6. Sketches of the four possible intermediates of **22**.

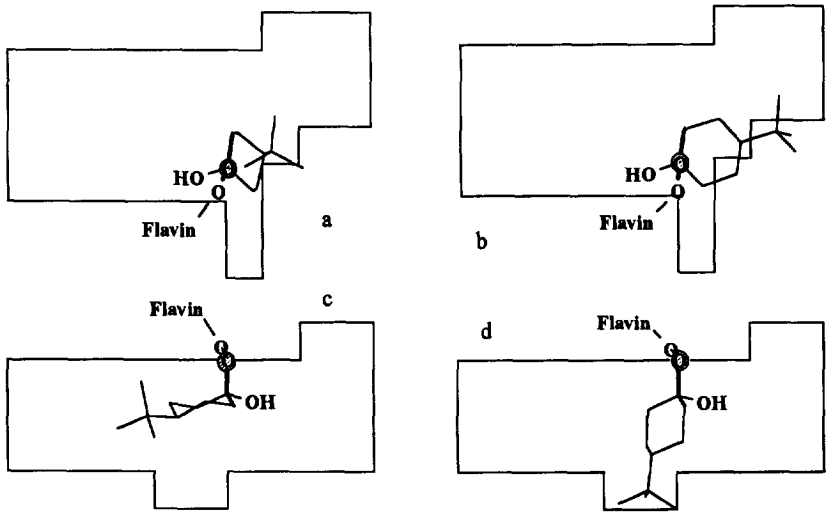

Figure 7. Sketches of the four possible intermediates of **32**.

in both cases the hydroxyl group points towards the inside of the M pocket and the intermediate structure lies partially outside the active site. In *b* it can also be seen that the flavin is in the axial position which is in disagreement with the model rules. Thus these two intermediates must be discarded. In part *c* (the intermediate which also gives the wrong product), the hydroxyl group is pointing correctly towards the H_S pocket with the

entire intermediate included inside the active site, but the flavin has an axial attachment. For the intermediate shown in part *d*, front view, the hydroxyl group points towards H_S and the attachment is equatorial, but the *t*-butyl group lies in the shaded area which was not included in the original active site model.

At this stage, the active site model developed for sulfoxidations appeared not to be suitable to predict CYMO stereochemistry with compound **32**. Only an enlargement of the lower part of the M pocket would have made it possible to accommodate the right intermediate (*d*) and therefore, this modification was introduced. In the case of compound **35** the results can not be explained with the model. It should be noted however, that the enantioselectivity of the enzyme for this substrate is only moderate (product ee 55%).

Miscellany

For compounds **17-20**, **25-28** and **36-38**, which do not belong to the previously examined groups, the stereochemical outcome was found to be consistent with the predictions made with the active site model.

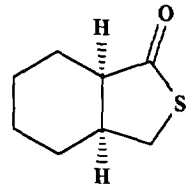

(1*R*,6*S*)-**39**

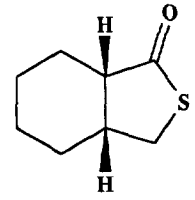

(1*S*,6*R*)-**40**

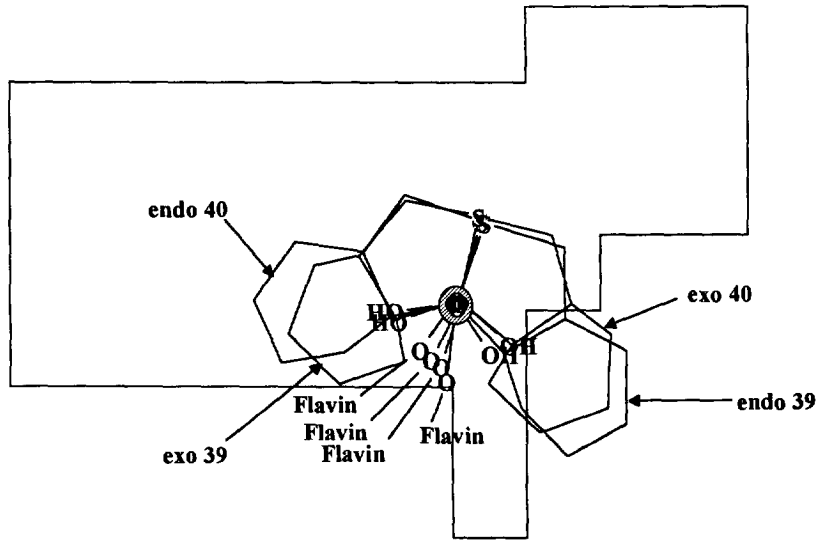

Figure 8. Sketches of four possible intermediates for inhibitors **39** and **40** for carbonyl attack.

Inhibition studies

Cyclic thiolactones are good substrate suicide-inhibitors. The inhibition mechanism is not completely understood yet since it is not known whether the enzyme attacks the carbonyl (Baeyer-Villiger oxidation) or attacks the sulfur (sulfoxidation).[14] Before the enantioselective inhibition studies with chiral bicyclic thiolactones,[15] any explanation of "normal" and "reverse" Baeyer-Villiger oxidation of bicyclo [n.2.0] ketones was questionable because the presence of isoenzymes with different catalytic behaviors could not be ruled out.

Figure 8 depicts the chiral thiolactones used for enantioselective inhibition studies. **Figure 8** also shows the four possible intermediates that can originate from a hypothetical carbonyl attack by the enzyme. It can easily be seen that only one intermediate for inhibitor can be formed with this model and that in one case **39** the attack to the carbonyl is exo whereas in the other case **40** the attack is endo. According to our rules, enantiomer **39** should be a better inhibitor than **40** and this agreed with the experimental results. Instead, if an attack to the sulfur is hypothesized, the model could not predict which enantiomer of **39** or **40** is more inhibitory.

Comparison with other models.

Other models that attempt to predict or rationalize the CYMO-catalyzed Baeyer-Villiger reactions have been reported in the literature. Furstoss'[4] and Taschner's[5] models have been amply discussed and compared with ours in a previous article,[7] and thus, they will not be further examined here. A third model has recently been proposed by Kelly's group,[6] and it classifies enzymes from different sources on the basis of the stereochemistry of the hydroxy peroxide intermediates. The Baeyer-Villiger reaction, as already mentioned, has precise stereoelectronic requirements and always proceeds via a chiral transition state and this is also true for pro-prochiral ketones[6]. Careful analysis of the Criegee intermediate for CYMO from *Acinetobacter* NCIMB 9871 showed an "*S*-migration configuration" when the Cahn-Ingold-Prelog rules were applied and when it was stated that the priority of the migrating group overcomes that of the non-migrating group.[6] This "*S*-migration configuration" using the usual rules for the trigonal centers also defined a *si*-face migration for the intermediate (**Scheme**). Instead, a similar enzyme, MO1 from *Pseudomonas putida* NCIMB 10007, showed an "*R*-migration configuration."[6]

A comparison of our model with Kelly's model for enantiomer *S,S*-**2**, gave straightforward results. **Figure 2,** part *a* and *d*, shows that the migration configuration is clearly *S*, whereas in part *b* and *c* it is *R*. On the basis of exo/endo considerations, the intermediate depicted in part *d* can be easily discarded and therefore, the same result is obtained with both models. With analogous reasoning, the intermediate of enantiomer *R,R*-**2** depicted in **Figure 3** part *a*, is the preferred one for both models. Although Kelly's model appears to be good for small molecules, it could make mistakes as the size of the substrates increases, because the bulkiness of the molecule will influence the reaction more and more. As an example, both structures shown in **Figure 4** should be productive because they have "*S*-migration configuration," but actually only the intermediate depicted in part *b* is (**Table I** entry **3**).

Conclusions.

The proposed active site model for CYMO was originally established for the sulfoxidation of sulfides and tentatively applied to a few Baeyer-Villiger oxidations. Using a wide range of ketones, it has now been shown that this model, after a minor refinement, is also able generally to predict the stereoselectivity of the Baeyer-Villiger reaction. In addition, this model sheds new light on enzymatic reverse Baeyer-Villiger oxidations and correctly assigns the right stereochemistry of the products. Inhibition studies can also take advantage of this active site model even though further work in this direction must be done. In addition, the model is consistent with and integrates the other models already described in the literature.

In conclusion, the proposed active site model for CYMO from *Acinetobacter* NCIMB 9871 can be used with confidence to predict the stereochemistry for both Baeyer-Villiger oxidation of ketones and sulfoxidation of sulfides.

Acknowledgements.

We are grateful to Dr. Veronique Alphand (CRNS Marseille) for providing us with her Baeyer-Villiger database. This work was partially supported by EEC Human Capital and Mobility Program.

References.

1. Baeyer, A.; Villiger, V.; *Ber. Dtsch. Chem. Ges.*, **1899**, *32*, 3625-3633.
2. a) Donoghue, N. A.; Norris, D. B.; Trudgill, P. W.; *Eur. J. Biochem.*, **1976**, *63*, 175-192. b) Schwab, J. M.; Li, W.-b.; Thomas, L. P.; *J. Am. Chem. Soc.*, **1983**, *105*, 4800-4808. c) Walsh, C. T., Chen, Y.-C. J.; *Angew. Chem. Int. Ed. Engl.*, **1988**, *27*, 33-343. d) Trudgill, P. W.; *Methods In Enzymology*, **1990**, *188*, 70-77.
3. Carrea, G.; Redigolo, B.; Riva, S.; Colonna, S.; Gaggero, N.; Battistel, E.; Bianchi, D.; *Tetrahedron: Asymmetry*, **1992**, *3*, 1063-1068.
4. Furstoss, R.; in *Microbial Reagents in Organic Synthesis*, S. Servi Ed. Kluwer Academic Publisher, **1992**, 333-346.
5. Taschner, M. J.; Pedadda, L.; Cyr, P.; Chen, Q.-Z.; Black, D. J.; in *Microbial Reagents in Organic Synthesis*, S. Servi Ed. Kluwer Academic Publisher, **1992**, 347-360.
6. a) Kelly, D. R.; Knowless, C. J.; Mahdi, J. G.; Taylor, I. N.; Wright, M. A.; *J. Chem. Soc., Chem. Commun.*, **1995**, 729-730. b) Kelly, D. R.; Knowles, C. J.; Mahdi, J. G.; Wright, M. A.; Taylor, I. N.; Hibbs, D. E.; Hursthouse, M. B.; Mish'al, A. K.; Roberts, S. M.; Wan, P. W. H.; Gogan, G.; Willetts, A. J.; *J. Chem Soc. Perkin Trans. 1*, **1995**, 2057-2066.
7. Ottolina, G.; Pasta, P.; Carrea, G.; Colonna, S.; Dallavalle, S.; Holland, H.L.; *Tetrahedron: Asymmetry*, **1995**, *6*, 1375-1386.

8. Alphand, V.; Archelas, A.; Furstoss, R.; *J. Org. Chem.*, **1990**, *55*, 347-350.

9. Sandey, H.; Willetts, A. J.; *Biotechnol. Lett.* **1992**, 1119-1125.

10.a) Jones, J.B.; Jakovac, I.J.; *Can. J. Chem.*, **1982**, *60*, 19-28. b) Toone, E.J.; Werth, M.J.; Jones, J.B.; *J. Am. Chem. Soc.*, **1990**, *112*, 4946-4952. c) Provencher, L.; Wynn, H.; Jones, J.B.; Krawczyk, A.R.; *Tetrahedron Asymmetry*, **1993**, *4*, 2025-2040. d) Provencher, L.; Jones, J.B.; *J. Org. Chem.*, **1994**, *59*, 2729-2732.

11. Noyori, R.; Kobayashi, H.; Sato, T.; *Tetrahedron Lett.*, **1980**, *21*, 2573-2576.

12. Deslongchamps, P.; in *Stereoelectronic effects in Organic Chemistry.* Pergamon Press, **1983**, 313-314.

13. HyperChem from HYPERCUBE INC. Waterloo, Ontario, Canada.

14. Latham, J. A.; Walsh, C.; *J. Am. Chem. Soc.*, **1987**, *109*, 3421-3427.

15. Wright, M.; Knowles, C.; Petit, F.; Furstoss, R.; *Biotechnol. Lett.*, **1994**, *16*, 1287-1292.

16. Lenn, M. J.; Knowles, C. J.; *Enzyme Microb. Technol.*, **1994**, *16*, 964-969.

17. Alphand, V.; Archelas, A.; Furstoss, R.; *Tetrahedron Lett.*, **1989**, *30*, 3663-3664.

18. Alphand, V.; Furstoss, R.; *J. Org. Chem.*, **1992**, *57*, 1306-1309.

19. Carnell, A. J.; Roberts, S. M.; Sik, V.; Willetts, A. J.; *J. Chem. Soc., Chem. Commun.*, **1990**, 1438-1439.

20. Carnell, A. J.; Roberts, S. M.; Sik, V.; Willetts, A. J.; *J. Chem. Soc., Perkin Trans. 1*, **1991**, 2385-2389.

21. Petit, F.; Furstoss, R.; *Tetrahedron: Asymmetry*, **1993**, *4*, 1341-1352.

22.Taschner, M. J.; Peddada, L.; *J. Chem. Soc., Chem. Commun.*, **1992**, 1384-1385.

23. a) Levitt, M. S.; Newton, R. F.; Roberts, S. M.; Willetts, A. J.; *J. Chem. Soc., Chem. Commun.*, **1990**, 619-620.

b) Willetts, A.J.; Knowles, C.J.; Levitt, M. S.; Roberts, S. M.; Sandey, H.; Shipston, N. F.; *J. Chem. Soc., Perkin Trans., 1* **1991**, 1608-1610.

24. Alphand, V.; Archelas, A.; Furstoss, R.; *Biocatalysis*, **1990**, *3*, 73-83.

25. Gagnon, R.; Grogan, G.; Groussain, E.; Pedragosa-Moreau, S.; Richardson, P. F.; Roberts, S. M.; Willetts, A. J.; Alphand, V.; Lebreton, J.; Furstoss, R.; *J. Chem Soc. Perkin Trans. 1*, **1995**, 2527-2528.

26. The authors used pure enantiomers. Alphand, V.; Furstoss, R.; *Tetrahedron: Asymmetry*, **1992**, *3*, 379-382.

27. Taschner, M. J.; Black, D. J.; *J. Am. Chem. Soc.*, **1988**, *110*, 6892-6893.

28. Taschner, M. J.; Black, D. J.; Chen, Q.-Z.; *Tetrahedron: Asymmetry*, **1993**, *4*, 1387-1390.

29. Taschner, M. J.; Chen, Q.-Z.; *Bioorg. Med. Chem. Lett.*, **1991**, *1*, 535-538.

(*Received in UK* 2 *February* 1996)